Comparing and Combining Underfoot Pressure Features for Shod and Unshod Gait Biometrics

Patrick C. Connor
ViTRAK Systems Inc.
Charlottetown, PE, C1A 1A5
Email: patrick@vitraksystems.com

***Abstract*—Underfoot pressure is becoming a fully-fledged gait biometric modality with the advent of modular, high-resolution sensing floor tiles because they capture rich gait signals without requiring the subject's cooperation. The literature on underfoot pressure-based gait recognition has posed a variety of features for both the barefoot and shod walking cases. In this paper, we compare and combine a large number of these with three use case scenarios in mind: 1) barefoot gait recognition and shod-foot recognition when the shoe used in training is 2) the same and 3) different from the test shoe. Our results show a difference in the types of features most useful in each scenario and their combination yields barefoot recognition (EER of 2.2%) that approaches the performance levels of biometrics currently in use, a good showing for this emerging technology.**

I. Introduction

Gait as a biometric has been studied over the last two decades. Although the younger cousin, relatively speaking, to fingerprint, iris, and face biometrics, gait is maturing in its reliability. A number of studies have reached correct identification rates in excess of 90% with 50+ subjects (e.g., [1]–[3]). Unlike fingerprint and iris biometrics, gait has the attractive properties of being accessible at a distance and not requiring the user's cooperation. Its unobtrusiveness also allows the silent capture of multiple gait instances and thereby avoids burdening the user should the first instance be inconclusive. Face biometrics share these properties, but are perhaps easier to hide or disguise. Whereas it is socially acceptable for the face to be covered, sheltered, or transformed by cosmetics and hairstyle, one must walk to move about, and doing so in an unnatural manner is less efficient and may arouse suspicion in public.

Underfoot pressure-based gait biometrics have a few benefits over their more popular video-based relative. In video, the environment (brightness, contrast, and shadows) can affect results, as seen in outdoor versus indoor effectiveness [4]. Viewpoint, occlusions, and background movement can affect extraction of the gait information, and variations in clothing or the carrying of objects can affect apparent body shape and may obscure the gait itself. Underfoot pressures, however, are the same whether indoor or outdoor, are independent of viewpoint (i.e., can be easily rotated), and rarely suffer from occlusions or background movement because of constant contact with the ground. Clothing and even the carrying of objects in a variety of scenarios appears to have a negligible effect [2]. These advantages allow underfoot pressures to be used for identification and tracking of multiple individuals simultaneously, which would support a variety of security applications. With the recent advent of modular high-resolution pressure-sensing floor tiles (Stepscan®, ViTRAK Systems Inc.), it becomes unnecessary to walk in a certain location or direction or to aim footfalls. This advancement enables underfoot pressure-based gait recognition to occur without user cooperation, as always enjoyed by its video-based counterpart.

Gait pressure data can be used to discriminate between individuals, especially when barefoot. One high-resolution underfoot pressure sensing approach achieved a 99.6% identification rate for 104 *barefoot* subjects. The primary challenge of underfoot pressure-based gait as a biometric is identifying feet transformed by variations in footwear. However, a large portion of the features from the literature on underfoot-pressure gait biometrics appear to be relatively shoe invariant. These include basic gait analysis features (e.g., stride length, toe-out angle), ground reaction force profile features, high-resolution pressure durations, and center of pressure features. Importantly, such features are either based on high-resolution pressure information or can be derived simply from it.

Fingerprint and iris-based biometrics are used effectively in practical applications because their associated algorithms rarely error. In this paper, we evaluate the reliability of underfoot pressure information to identify or track subjects. We first review the literature's best performing underfoot-pressure features and explain how they are extracted from high-resolution pressure data. Then, we evaluate both the identification and verification tasks on underfoot pressure data for the features described, in several application-focused scenarios. The key contribution of the present work is to determine the best performing of these features (and combinations thereof) in each scenario, which is valuable information for moving the technology toward commercialization. This is the first time an evaluation among such a wide variety of underfoot pressure features has been undertaken.

II. Background

Gait recognition is appreciated for its ability to identify individuals at a distance without their cooperation. A plethora of video-based approaches have been proposed since an inaugural paper in 1994 by Niyogi and Adelson [5]. Some give very high identification rates for substantial numbers of subjects. For example, Lee and Grimson [6] achieved a 100% classification rate (CR) for 25 subjects using features derived from ellipses fitted to the individual. Seely et al. [1] achieved a CR of 99.6% (103 subjects) using averaged and centered silhouettes from multiple views over a gait sequence as features. Yoo and Nixon [7] fitted a 8-segment skeletal model to a dataset of gait video

978-1-4799-1737-2/15/$31.00 ©2015 IEEE

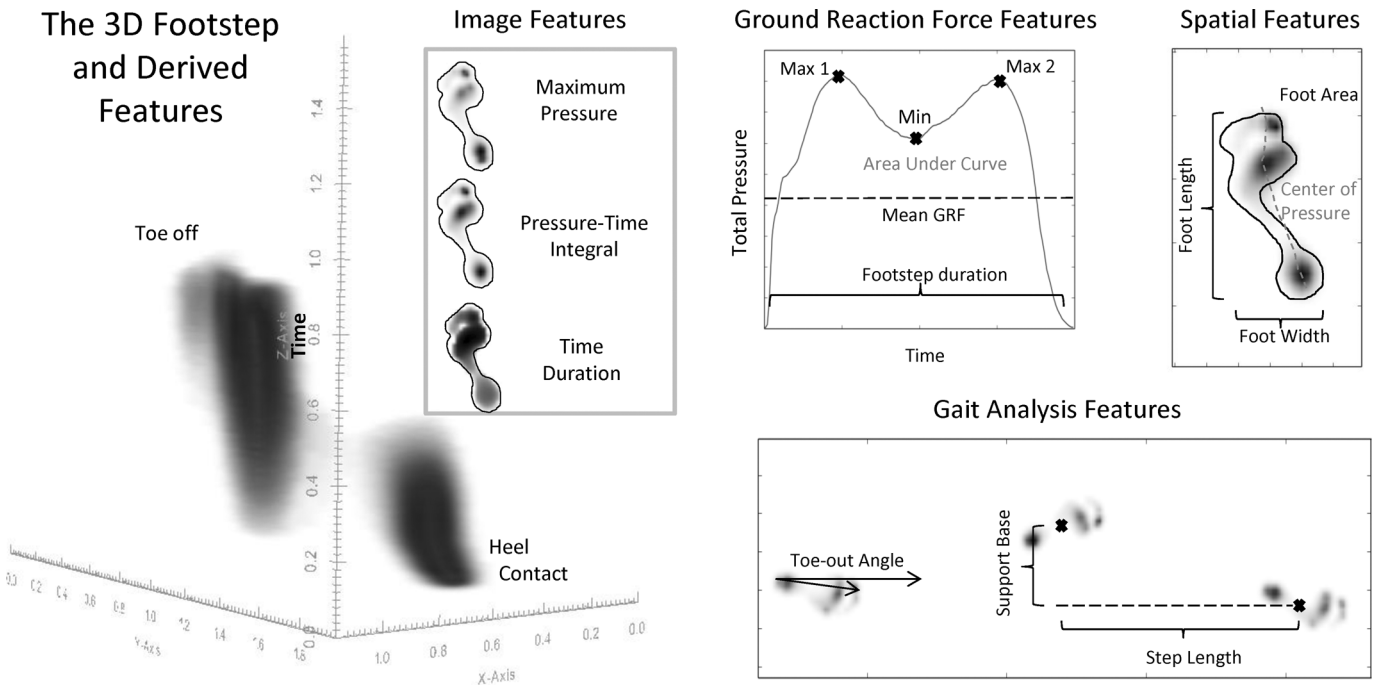

Fig. 1. Three-dimensional underfoot pressures and features derived from them. The 2D sensor grid reads pressure at 100 Hz, providing a 3D volume of information. From this, several 2D image representations can be computed as well as specific spatial features. The 3D volume can also be reduced to a 1D signal, total pressure over time, to extract ground reaction force features. Gait analysis features capture relationships between footsteps.

sequences. They extracted height, gait analysis features (cycle time, stride length, speed), and several dynamic angular and position related features to a achieve 96.7% CR on a dataset of 30 subjects and an 84.0% CR on a dataset of 100 subjects. Unfortunately, however, results decline in lesser controlled environments. The Gait Challenge datasets [8], [9] capture gait in varying circumstances including covariates of footwear, walking surface, carrying condition, and time, showing varying and heavily declining rates (tens of percent) as conditions deviate from a standard. Even Lee and Grimson's classification rates plummeted to between 40% and 50% when the test data came from a subsequent day of recording. Several studies have attempted to address these and other covariates including walking speed [7], [10] and camera viewpoint [11]. Perhaps the most challenging covariate yet to be effectively addressed in video-based gait recognition is clothing [12], which often changes between recording sessions.

Underfoot pressure-based gait recognition approaches have also proven effective. Pataky et al. [3], recording on a high-resolution pressure mat, achieved a 99.6% CR (104 barefoot subjects) based on a subset of 2D image features derived from the 3D footprint (2D pressures over time). ~~Jung et al. [13]~~, computed an averaged binary silhouette called the "Footprint Energy Image" of a left-right pair of footsteps and achieved a CR of 96.2% (26 subjects). This extended earlier work [14], which used a binary image of the left-right pair and achieved a 91.4% CR (11 subjects). This earlier work also proposed using the center of pressure (COP) X-Y position over time as a vector features, which achieved a 79.6% CR (11 subjects). All of these studies used barefoot data. In most public settings, however, people wear shoes. While underfoot pressures may be unaffected by changes in clothing, changes in footwear appears to be the primary covariate to overcome.

Conveniently, many early approaches to identification based on underfoot pressures used force plates, which acquire a single pressure signal over time per footstep. These "ground reaction force" (GRF) signals do not capture spatial information like the 2D image features, but rather rely on temporal changes in pressure alone. Orr and Abowd [15] extracted key point features from the peaks and valleys of the GRF's typical "M" shape, as shown in Figure 1. They also captured footstep duration, total area under the pressure curve, and the pressure mean (a measure of mass) and standard deviation. Altogether, these features gave a best CR of 93% (15 subjects). In Orr and Abowd's study, some subjects wore several pairs of shoes, suggesting that it is possible to learn to recognize people from underfoot pressures even with changes in footwear. Though footwear may obscure spatial information to some degree, this result suggests that it does not affect temporal information substantially. Moustakidis et al. [2], [16] extracted wavelet packet (WP) features from GRF profiles. These capture a more holistic view of the GRF than do the manually extracted features described above. In their studies, the footwear covariate was not tested (subjects wore their own footwear), but walking speed (low, normal, and high speed) and carrying up to 10% of the subject's body mass (right hand, left hand, both, and backpack) were evaluated. With randomly selected training and test sets comprised of all covariates a CR of 98.2% (40 subjects) was obtained. Carrying condition had negligible effects whereas walking speed reduced rates

978-1-4799-1737-2/15/$31.00 ©2015 IEEE

significantly (by as much as 15%), but was overcome by including data from several walking speeds in the training set. From comparisons with tests on the same data using manually extracted features, they found their WP approach to be much less affected by these covariates.

Basic foot size and gait analysis-based features also appear to be relatively footwear invariant. Middleton et al. [17] used stride length, single step period (a form of walking speed), and the ratio of time spent on the heel vs. time spent on the toes as features. Together, these features gave an 80% CR (15 subjects), with the last feature alone achieving 60%. BenAbdelkader et al. [18] achieved CRs of 18% and 51% (41 and 17 subjects, respectively) when identifying by stride length and cadence (footsteps/minute). Adding height, which is a correlate of foot length, improved these results to 47% and 65%, respectively. Takeda et al. [19] extracted foot width, length, and angle (i.e., toe-out angle) among other features, but did not report a CR on these features alone.

III. Data Acquisition and Preprocessing

In this work, we use two novel and openly available datasets, both associated with the CASIA gait recognition database D [20], [21]. The barefoot walking dataset consists of 92 subjects (mostly male, between the ages of 21 and 57) who walked across a commercial pressure mat (255 x 64 pressure sensors, 2096 mm x 469 mm, 100 Hz) and provided 25 or more footsteps each over 10 trials. Approximately half of the footsteps were recorded at a natural walking pace and half at a fast pace. The shod walking dataset consists of 15 subjects (demographics unknown) with 25+ shod footprints, and 13 of these subjects also gave 25+ shod footprints in a second pair of shoes. There is substantial variety in the forms of footwear, which include dress shoes, trainers, slippers, and high heels. All subjects are from various parts of mainland China. From each recording session, single 3D footsteps were extracted, harvesting a total of 2300 footsteps in the barefoot dataset and 700 footsteps in the shod dataset. Each volume (60x40x100 voxels) contains a single complete footstep. Partial footsteps were excluded from analysis and any other footsteps (full or partial) within the same volume were separated out. This "raw" data, was also aligned in the X and Y dimensions to either an average healthy foot (Munster 104 Template [22]) for barefoot data or a custom template for shod data. We used the same footstep alignment procedure [23] that was used to achieve the highly accurate results in [3]. The aligned dataset was also normalized for walking speed and apparent mass to avoid potential distortion of the unique gait features by these easily varied elements. To normalize for walking speed, our aligned 3D data is resampled with nearest neighbour interpolation to stretch footsteps to 100 samples in time. To normalize for mass, we divide each aligned 3D pressure value by the average of its footstep's GRF profile. Mass and footstep duration are themselves evaluated as potential features.

From these shod and unshod datasets, we consider three application scenarios. In the "barefoot" scenario, a recognition system sees and evaluates (classifies) only barefoot data, which has typically given the highest recognition rates in the literature and may be appropriate for high-level security, such as may be required in an airport setting. In the "same shoe" scenario, the system sees and evaluates footsteps where subjects wear the same footwear throughout. This is appropriate for subject tracking, since individuals are unlikely to switch footwear while in transit. Finally, in the "different shoe" scenario, the system sees examples of individuals walking in one pair of footwear and evaluates footsteps when they wear a second pair of footwear. This is a very challenging problem, but a natural use case since people often wear more than one pair of shoes on a regular basis. This may be more appropriate for internal security/tracking such as identifying employees as they access controlled areas on the interior of a company facility.

IV. Underfoot Pressures Feature Extraction

Figure 1 illustrates the variety in features that can be extracted from the raw or aligned datasets. The aligned data itself can be used as a feature set. However, it has a large number of features (i.e., voxels), which will have a generally negative effect during classification when the training dataset is small (i.e., the "curse of dimensionality"). A standard way of addressing this is to employ Principal Components Analysis (PCA) which finds a transformation of the data where the high-dimensional axes are oriented along the direction of covariation between feature values (i.e., the eigenvectors of the covariance matrix). The data is then projected onto the most covarying of these axes (i.e., the principal axes) and this projection is used as the feature set for classification. This process tends to capture the majority of the original information in the data but with far fewer features. We apply this approach to the aligned footstep data.

2D Image Features. In Pataky et al. [3], the 3D volumes were collapsed into distinguishing 2D images in several ways. Image features from their work that we evaluate here include the maximum pressure and pressure-time integral (PTI) image features based on the aligned data. The maximum pressure features are simply the maximum pressure over time at each X-Y location and the PTI features are merely the sums of pressures over time at each location. We also consider pressure duration or the "footprint energy image", as computed by Cho et al. [24], which is the sum of the footstep binary silhouettes (non-zero pressure values = 1) over time at each x-y location. Pataky et al. also employ these duration image features.

Spatial Features. For basic spatial features, we compute the foot length, width, and area from the binary silhouette of the maximum pressure image as the largest count of pixels in the appropriate dimension and the sum for area. The COP trajectory is computed as the sum of image positions weighted by their respective pressures in each time slice in the aligned dataset. The COP principal components are used as features. We also compute WP features from the COP (X and Y COPs separately) because of the similarity between the GRF and COP curves. We also compute Middleton et al. [17]'s ratio of time spent on the heel versus time spent on the toe. The approximate heel and toe positions are set to the COP locations at frames 10 and 90 in aligned footprint, respectively. The time duration of each is the count of non-zero pressures at their respective x-y locations over time.

Ground Reaction Force Features. The vertical GRF profile is computed as the sum of pressures from a single footstep at each time instant, derived from the aligned dataset. From this, we derive several feature representations for evaluation. One

978-1-4799-1737-2/15/$31.00 ©2015 IEEE

is the set of manually extracted features of Orr and Abowd described above. We also take GRF principal components as features (i.e., PCA), a strategy used by Vera-Rodríguez et al. [25], [26]. The last way we represent the GRF signal is by using the WP decomposition algorithm of Moustakidis et al. [2]. Our implementation differs in that we used the Biorthogonal (1.5) wavelet instead of the Coiflet wavelet because it gave generally better CRs in preliminary testing on our data.

Gait Analysis Features. These features include the toe-out angle, cadence, walking or support base, and step length. The toe-out angle associated with each footstep is taken as the angle used to align the raw footprint to its associated template. This approach assumes that subjects walk parallel to the edge of the walkway used to collect the data. The step length and support base are computed as the length and width in pixels between the approximate center of one foot and the center of an adjacent (and opposite) foot in the gait cycle, respectively. Though only calculable with two footsteps, these measures are assigned to each footstep to allow comparisons with the other features, which are provided per footstep.

V. Results

In our evaluation, we sought to find out which features and feature combinations worked best in each of the three application scenarios. We also aimed to determine the best performance we could achieve in each scenario by combining multiple features. Common to both of these goals is the task of classification. For the "barefoot" and "same shoe" application scenarios, we used 25-fold cross validation. That is, we "trained" a nearest neighbour classifier on 24 of the 25 footstep samples for each subject and classified (tested) the 25th one, for every possible combination of 24+1 samples (i.e., 25 times). The "different shoe" scenario is trained on the same data as the same shoe scenario (minus 2 subjects not recorded for 2 pairs of shoes), but is tested on 25 footsteps with the second pair of footwear for each of the 25 training sets. Like many other gait recognition studies, we chose the nearest neighbours classifier for the present study since it is simple, efficient, and easily interpretable. This classifier also allowed us to avoid evaluating left and right foot data separately because they will naturally separate into different regions of feature space if different and not be confused or averaged. We evaluated both the identification classification problem (i.e., as many classes as subjects) and the verification classification problem (i.e., two classes for either acceptance or rejection as the claimed identity).

To assess the discriminative ability of each feature in each application scenario, we used the identification classification problem and forward feature selection. First, we classified test footsteps based on every feature separately in each scenario, as shown in Table I under the heading SCR for solo classification rate (percent). This expresses how much discriminative ability is in each feature. Only results for the best half of the features are listed, justified further below. Principal components and WP features are grouped in sets of 5 features each, where each is weighted by $\frac{1}{5}$ so that each group has the same weight as a single feature. The weights are passed into the nearest neighbours classifier to weight the influence of each dimension in the distance measure accordingly. The group size of 5 was chosen to maximize CRs and yet report results succinctly and meaningfully.

Many of the features contain overlapping information, so to find effective combinations that contain the most complete set of discriminative information, we use forward feature selection. In this procedure, the most discriminative feature is first found (i.e., highest solo classification rate). Then, this feature is combined with every remaining feature in turn to find the best performing combination of two features. A third feature is added in the same way, and so on, until the best classification rate is achieved, which will often occur before all of the features are added. The order in which features were added for each application scenario is listed in the "Rank" columns of Table I, which include all of the best features (in bold) used to reach the highest CRs in each scenario.

Although the exact solo CRs and "ranking" of the features will be somewhat data dependent, we can see some general trends. Roughly speaking, the barefoot data is best classified with the 2D image features and COP information. Features from gait analysis and GRFs are mostly inferior in this scenario, perhaps in part due to the data containing two different walking speeds. In the "same shoe" scenario, the image features are still useful as are the aligned data features, but there is a rise in the importance of the gait analysis and simple spatial features. Their importance increases still further in the "different shoe" scenario, where the 2D image and aligned data features become secondary. The one exception to this is the first group of principal components of the duration image, which achieve the second highest solo CR in this application scenario. Across all scenarios, the COP information is helpful and in particular a portion of the COP along the y-axis. The features derived from the GRF profile are not especially effective in general, contrary to the strong GRF WP results of Moustakidis et al. [2]. This does not appear due to weakness in our WP feature extraction implementation since certain COP WP features are among the most discriminative.

The performance for the best combination of features in each footwear scenario is given in Table II. The dominance of the same shoe scenario results is partly due to having far fewer subjects than the barefoot scenario. The challenging different shoe scenario, as expected, has the lowest performance. For applications where the users are a closed (known) group of individuals, the CR, False Acceptance Rate (FAR) and False Rejection Rate (FRR) in Table II are appropriate measures because classification decisions are based on the closest footstep match in the database. An FAR of 1% means that someone seeking to be identified as another known user will be successful 1% of the time, and an FRR of 10% says that someone will be unsuccessful in attempting to be identified as themselves 10% of the time. FRRs in the tables express the degree to which one's footsteps appear more like someone else's in the database. For applications with the potential for unknown users (an open user group), the detection error tradeoff (DET) graph shown in Figure 2 is more appropriate. It depicts the FAR and FRR as well, but as a function of a moving decision boundary or threshold, rather than according to the closest footstep match in the database. The equal error rate (EER) in the graph and tables is derived from the DET curve, the point where the FAR and FRR are equal.

In a straightforward identification/verification application,

978-1-4799-1737-2/15/$31.00 ©2015 IEEE

TABLE I. RELATIVE FEATURE EFFECTIVENESS FOR VARIOUS FOOTWEAR APPLICATION SCENARIOS.

Feature Name	Barefoot		Same Shoe		Diff. Shoe	
	Rank	**SCR**	**Rank**	**SCR**	**Rank**	**SCR**
Align. D. PCs (0-4)	42	26.4	14	79.2	54	20.5
Align. D. PCs (5-9)	**33**	26.7	**2**	78.9	**12**	20.3
Align. D. PCs (10-14)	56	15.2	**5**	58.7	67	15.5
Max Im. PCs (0-4)	**23**	23.9	**1**	82.7	42	20.3
Max Im. PCs (10-14)	**9**	16.2	14	60.5	45	16
Max Im. PCs (15-19)	**2**	19	15	53.9	51	6.08
Max Im. PCs (20-24)	**17**	13.1	20	45.9	40	6.18
Max Im. PCs (25-29)	**29**	13.7	19	41.9	69	9.23
Max Im. PCs (30-34)	**31**	10.7	17	31.7	26	11.2
Max Im. PCs (35-39)	36	9.96	15	25.6	90	8.01
Max Im. PCs (40-44)	**15**	8.52	16	24.3	**20**	9.87
Max Im. PCs (45-49)	**21**	6.65	37	15.5	30	7.2
PTI Im. PCs (0-4)	**1**	28	15	82.1	49	18.4
PTI Im. PCs (5-9)	**20**	25.3	**6**	70.1	68	13.5
PTI Im. PCs (10-14)	**33**	15.7	**5**	65.9	**13**	12.6
PTI Im. PCs (15-19)	**26**	15.3	22	45.3	**17**	12.4
PTI Im. PCs (30-34)	**32**	9.3	14	27.7	76	9.24
PTI Im. PCs (35-39)	**16**	6.48	52	23.2	84	9.9
PTI Im. PCs (45-49)	**23**	5.48	54	13.3	109	8.71
Dur. Im. PCs (0-4)	51	18.8	21	63.7	**3**	37.5
Dur. Im. PCs (5-9)	**27**	12.9	12	47.2	50	21.3
Dur. Im. PCs (10-14)	**6**	9.43	17	29.6	**18**	18.8
Dur. Im. PCs (15-19)	**19**	7.3	16	28.5	34	11.1
Dur. Im. PCs (20-24)	**34**	4.61	26	26.1	35	12.4
Dur. Im. PCs (25-29)	**18**	6.17	16	21.6	98	11.3
Dur. Im. PCs (30-34)	64	3.96	20	17.3	**19**	13.7
COPx WP (65-69)	91	1.78	21	12.8	**9**	20.9
COPy WP (30-34)	65	1.35	118	9.6	**21**	14.6
COPy WP (50-54)	**13**	13	**4**	63.7	**1**	41.2
COPy WP (55-59)	**10**	8.3	16	38.7	**11**	19.7
COPy WP (65-69)	92	7.52	94	29.1	**23**	15.3
COPxy PCs (0-4)	37	26.7	**1**	82.7	59	27.7
COPxy PCS (5-9)	**3**	27.7	20	75.5	25	22.3
COPxy PCs (10-14)	**25**	18.3	13	67.5	87	7.35
COPxy PCs (15-19)	**17**	16.2	11	52	113	12.5
COPxy PCs (20-24)	**11**	14.7	20	50.7	106	10.7
COPxy PCs (25-29)	**4**	14.5	20	31.5	38	12.7
COPxy PCs (30-34)	**8**	13.5	20	36.3	**16**	7.08
COPxy PCs (35-39)	**5**	11	16	22.9	93	8.78
Foot length	**14**	4.39	**5**	22.4	**6**	2.81
Foot width	**30**	2	15	18.9	100	3.69
Foot area	**7**	6.57	**5**	40.8	96	18.5
GRF mean (mass)	85	1.39	17	15.5	27	16.6
GRF std	63	1.74	39	20.3	**7**	17.3
GRF duration	74	2.48	**7**	22.1	**8**	26
GRF max 1 val	**22**	1.09	131	6.67	127	7.69
GRF max 2 time	84	2.09	92	18.9	**14**	17.7
GRF min time	119	2.13	92	19.5	**15**	17.7
GRF WP (0-4)	50	2.83	24	23.7	63	7.77
GRF WP (5-9)	70	2.91	81	21.6	**22**	9.49
GRF PCs (0-4)	**12**	3.39	13	9.87	94	5.49
GRF PCs (5-9)	**35**	2.65	110	6.93	125	7.85
Step length	52	3.52	22	21.1	**4**	22.9
Support base	46	2.7	17	17.1	**10**	17.1
Cadence	56	2.57	**3**	22.9	**2**	26.7
Toeout	66	2.09	8	6.4	**5**	9.59

TABLE II. IDENTIFICATION AND VERIFICATION RATES IN VARIOUS FOOTWEAR SCENARIOS.

Footwear Scenario	**CR%**	**FAR%**	**FRR%**	**EER%**
Barefoot	93.2	0.0745	6.78	6.13
Same Shoe	100	0.0	0.0	2.13
Diff. Shoe	90.5	0.791	9.49	15.9

acquiring several footsteps as a user approaches a secure entrance seems quite reasonable. Basing a classification decision on multiple footsteps greatly improves test results for both the barefoot scenario and to a lesser degree for the different shoe scenario, as shown in Tables III and IV, respectively. Each of the multiple test footsteps is first classified separately and given a confidence score. The class that is most frequently chosen becomes the class for the group of footsteps. The highest cumulative score is used to break ties. To make this evaluation possible for the barefoot scenario, 4 footsteps were siphoned

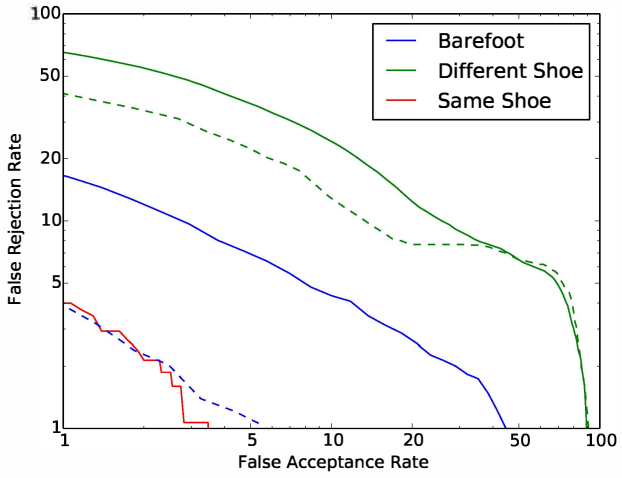

Fig. 2. Detection error tradeoff curve for the barefoot, same shoe, and different shoe scenarios. The DET curves for when five footsteps are used to perform classification are shown in dashed lines of corresponding color for the barefoot and different shoe scenarios.

from each training set into the corresponding test set, but after principal components and WP features were computed. Multi-footstep results for the barefoot and different shoe scenarios based on five test footsteps are also depicted in the DET graph of Figure 2 using dashed lines of the corresponding colour.

TABLE III. IDENTIFICATION AND VERIFICATION RATES BASED ON MULTIPLE BAREFOOT FOOTSTEPS.

No. Footsteps	**CR%**	**FAR%**	**FRR%**	**EER%**
1	91.3	0.0951	8.65	7.11
2	97.0	0.0325	2.96	4.06
3	98.9	0.000956	3.48	3.38
4	99.7	0.0	1.17	2.32
5	99.8	0	2.09	2.19

TABLE IV. IDENTIFICATION AND VERIFICATION RATES BASED ON MULTIPLE FOOTSTEPS WEARING A SHOE THAT IS DIFFERENT FROM THE SHOE WORN IN THE TRAINING DATA.

No. Footsteps	**CR%**	**FAR%**	**FRR%**	**EER%**
1	90.5	0.791	9.49	15.9
2	91.9	0.679	8.15	14.2
3	97.5	0.0641	3.96	13.0
4	97.6	0.141	4.51	12.6
5	99.5	0.00513	2.40	11.4

The same shoe scenario is applicable to multiple subject tracking, where the CR is most relevant. In tracking, however, there is initially only one or a few footsteps from which to classify future steps. Figure 3 shows how the classification rate increases as the number of same-shod steps in the training set increases. Even after only a few steps, the correct classification rate of the "next" step (for 15 simultaneously tracked subjects) is above 90% in spite of 5 of the 13 subjects wearing similar dress shoes and 2-3 others wearing slippers. Adding the ability to test on multiple next footsteps further boosts this result, as also shown in Figure 3.

The barefoot and different shoe scenario results are more statistically reliable than the same shoe scenario results. According to the "rule of 30" [27], the 90% confidence interval on the expected error rate is within $\pm 30\%$ of the observed

978-1-4799-1737-2/15/$31.00 ©2015 IEEE

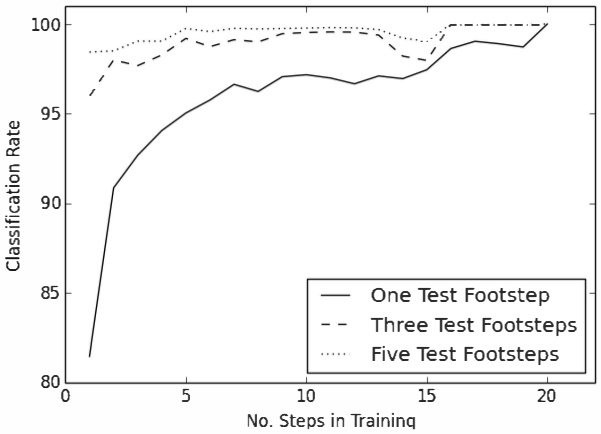

Fig. 3. CRs for one, three, or five test footsteps after training on a given number of previous steps (same shoe scenario).

error rate provided there are enough data samples to give 30 errors at the observed rate. In the case of the barefoot data there are 2300 data samples. At an observed EER of 2.19%, the number of errors is 50, which more than satisfies the rule of 30, giving an expected error between 1.53% and 2.85%. In the different shoe scenario, the rule of 30 also holds for its lowest EER of 11.4% (37 errors), giving an expected error between 8.0% and 14.8%. The same shoe scenario's low EER with few data samples, however, does not allow us to draw as statistically strong conclusions, not satisfying the rule of 30 (only 8 errors for an EER of 2.13% and 375 data samples). Although commonly used, we note that the "rule of 30" assumes that the within-class data samples are independent, and can therefore underestimate the number of samples needed for the desired confidence interval.

VI. Discussion

The overall gait recognition results here are encouraging and, in the barefoot case, approaching the level of high-performance fingerprint and iris biometrics, which achieve verification rates below 1% EER, 0.01% FAR, and 5% FRR [28], [29], iris recognition being the better performer. In spite of these positive results, better barefoot results were expected given the high classification accuracy of Pataky et al. [3], which also evaluates performance for large numbers of barefoot subjects. In Pataky's work, the maximum pressure image features scored an over 98% CR on their own, but even when employing all but a small (and less informative) portion of these features in the present work, we achieve only 93%. The difference may be in the data. Unlike Pataky's dataset, our barefoot dataset included samples from a normal and fast speed for each subject, which although more characteristic of the real world could be adding confusion during classification in spite of our attempts to normalize for it. Pataky's data was also recorded at a slightly finer resolution (5mm) than our data and recorded subjects with a different ethnic distribution (from Germany versus mainland China), which can influence the parameters of one's gait [30], [31]. For the same shoe scenario, we see results comparable to Jung et al. [13] and Moustakidis et al. [2], although they were achieved using different features. In the same shoe and different shoe scenarios, we achieved EERs similar to Takeda et al. [19]. It is difficult to say which results are superior because they are based on different datasets that are both small.

The feature extraction and classification methods can *test* multiple footprints per second at present with a single thread of processing. An additional time expense is in computing the WP decomposition and principal components axes by which the final features are computed. These, however, can be done offline after collection of a sufficient amount of preliminary data, perhaps even packaged with production software. Also, the time spent detecting and extracting footprints will be dependent on the sensor hardware and the sampling rate.

VII. Conclusions and Future Work

The present work has compared the effectiveness of different underfoot pressure features in several application-focused scenarios. With increased similarity between footprint appearance in the training and test data, the more reliance there will be on image features. The more dissimilar they are, the more useful GRF and gait analysis features become. Using forward feature selection to find the best features for each scenario, we have shown that underfoot pressure features are especially discriminative in the barefoot scenario, yielding an EER of 6.13% (92 subjects), and, in the tracking of multiple shod subjects, a CR above 90% (13 subjects) with only a few initial steps on which to train. These results are substantially bolstered (to 2.19% EER and >95% CR) by the ability to involve multiple footsteps in a single identification/verification without further burdening the subject, unlike other biometric approaches which require their cooperation. Even the FAR and FRR of the different shoe scenario improved dramatically, bringing it within the reach of some security applications.

To further improve our findings and bring underfoot pressure gait biometrics closer to commercialization, we propose several items of future work. First, it is appropriate to evaluate the use of more sophisticated classifiers which may better distinguish between subjects. Next, video-based gait information likely contains a substantially non-overlapping amount of information and appears relatively unaffected by most footwear [12]. Thus, fusion with video-based gait features, such as done by Zheng et al. [21], is expected to improve identification performance, especially in shod contexts. Our shod results are based on small datasets. To affirm the shod results, we feel there is value in acquiring a substantially larger dataset with a standard shoe as one footwear and the subject's own footwear as the second pair. This would also allow us to study the differences within and between shoe types and perhaps lead to novel features, such as proposed by Jung et al. [13], to better tackle the challenging different shoe scenario. There is little known about the stability of gait biometrics over time, although reports in the literature so far have been promising [3], [32]. Gait impersonation also deserves further study, although research so far suggests it is very difficult to mimic another's gait, even with substantial training [33], [34].

Acknowledgments

This research was supported in part by an NSERC IRDF grant. The author thanks Shuai Zheng for the barefoot and shod spatiotemporal footstep recordings used in this study.

978-1-4799-1737-2/15/$31.00 ©2015 IEEE

REFERENCES

[1] R. D. Seely, S. Samangooei, M. Lee, J. N. Carter, and M. S. Nixon, "The university of southampton multi-biometric tunnel and introducing a novel 3d gait dataset," in *Biometrics: Theory, Applications and Systems, 2008. BTAS 2008. 2nd IEEE International Conference on*. IEEE, 2008, pp. 1–6.

[2] S. Moustakidis, J. Theocharis, and G. Giakas, "Feature extraction based on a fuzzy complementary criterion for gait recognition using GRF signals," in *Control and Automation, 2009. MED'09. 17th Mediterranean Conference on*. IEEE, 2009, pp. 1456–1461.

[3] T. C. Pataky, T. Mu, K. Bosch, D. Rosenbaum, and J. Y. Goulermas, "Gait recognition: highly unique dynamic plantar pressure patterns among 104 individuals," *Journal of The Royal Society Interface*, p. rsif20110430, 2011.

[4] D. K. Wagg and M. S. Nixon, "On automated model-based extraction and analysis of gait," in *Automatic Face and Gesture Recognition, 2004. Proceedings. Sixth IEEE International Conference on*. IEEE, 2004, pp. 11–16.

[5] S. A. Niyogi and E. H. Adelson, "Analyzing and recognizing walking figures in XYT," in *Computer Vision and Pattern Recognition, 1994. Proceedings CVPR'94., 1994 IEEE Computer Society Conference on*. IEEE, 1994, pp. 469–474.

[6] L. Lee and W. E. L. Grimson, "Gait analysis for recognition and classification," in *Automatic Face and Gesture Recognition, 2002. Proceedings. Fifth IEEE International Conference on*. IEEE, 2002, pp. 148–155.

[7] J.-H. Yoo and M. S. Nixon, "Automated markerless analysis of human gait motion for recognition and classification," *ETRI Journal*, vol. 33, no. 2, pp. 259–266, 2011.

[8] P. J. Phillips, S. Sarkar, I. Robledo, P. Grother, and K. Bowyer, "The gait identification challenge problem: data sets and baseline algorithm," in *Pattern Recognition, 2002. Proceedings. 16th International Conference on*, vol. 1. IEEE, 2002, pp. 385–388.

[9] S. Sarkar, P. J. Phillips, Z. Liu, I. R. Vega, P. Grother, and K. W. Bowyer, "The HumanID gait challenge problem: Data sets, performance, and analysis," *Pattern Analysis and Machine Intelligence, IEEE Transactions on*, vol. 27, no. 2, pp. 162–177, 2005.

[10] S. Lee, Y. Liu, and R. T. Collins, "Shape variation-based frieze pattern for robust gait recognition," in *CVPR*, 2007.

[11] M. Goffredo, I. Bouchrika, J. N. Carter, and M. S. Nixon, "Self-calibrating view-invariant gait biometrics," *Systems, Man, and Cybernetics, Part B: Cybernetics, IEEE Transactions on*, vol. 40, no. 4, pp. 997–1008, 2010.

[12] I. Bouchrika and M. S. Nixon, "Exploratory factor analysis of gait recognition," in *Automatic Face & Gesture Recognition, 2008. FG'08. 8th IEEE International Conference on*. IEEE, 2008, pp. 1–6.

[13] J.-W. Jung, Y.-O. Cho, and B.-C. So, "Footprint recognition using footprint energy image," *Sensor Letters*, vol. 10, no. 5-6, pp. 1294–1301, 2012.

[14] J.-W. Jung, S.-W. Lee, Z. Bien, and T. Sato, "Person recognition method using sequential walking footprints via overlapped foot shape and center-of-pressure trajectory," *IEICE Transactions on Fundamentals of Electronics, Communications and Computer Sciences*, vol. 87, no. 6, pp. 1393–1400, 2004.

[15] R. J. Orr and G. D. Abowd, "The smart floor: a mechanism for natural user identification and tracking," in *CHI'00 extended abstracts on Human factors in computing systems*. ACM, 2000, pp. 275–276.

[16] S. P. Moustakidis, J. B. Theocharis, and G. Giakas, "Subject recognition based on ground reaction force measurements of gait signals," *Systems, Man, and Cybernetics, Part B: Cybernetics, IEEE Transactions on*, vol. 38, no. 6, pp. 1476–1485, 2008.

[17] L. Middleton, A. A. Buss, A. Bazin, and M. S. Nixon, "A floor sensor system for gait recognition," in *Automatic Identification Advanced Technologies, 2005. Fourth IEEE Workshop on*. IEEE, 2005, pp. 171–176.

[18] C. BenAbdelkader, R. Cutler, and L. Davis, "View-invariant estimation of height and stride for gait recognition," in *Biometric Authentication*. Springer, 2002, pp. 155–167.

[19] T. Takeda, K. Kuramoto, S. Kobashi, and Y. Hata, "A challenge to biometrics by sole pressure while walking," in *Fuzzy Systems (FUZZ), 2011 IEEE International Conference on*. IEEE, 2011, pp. 1430–1435.

[20] S. Zheng, K. Huang, and T. Tan, "Evaluation framework on translation-invariant representation for cumulative foot pressure image," in *Image Processing (ICIP), 2011 18th IEEE International Conference on*. IEEE, 2011, pp. 201–204.

[21] S. Zheng, K. Huang, T. Tan, and D. Tao, "A cascade fusion scheme for gait and cumulative foot pressure image recognition," *Pattern Recognition*, vol. 45, no. 10, pp. 3603–3610, 2012.

[22] T. C. Pataky, K. Bosch, T. Mu, N. L. Keijsers, V. Segers, D. Rosenbaum, and J. Y. Goulermas, "An anatomically unbiased foot template for inter-subject plantar pressure evaluation," *Gait & posture*, vol. 33, no. 3, pp. 418–422, 2011.

[23] F. P. Oliveira, T. C. Pataky, and J. M. R. Tavares, "Registration of pedobarographic image data in the frequency domain," *Computer methods in biomechanics and biomedical engineering*, vol. 13, no. 6, pp. 731–740, 2010.

[24] Y.-O. Cho, B.-C. So, and J.-W. Jung, "User recognition using sequential footprints under shoes based on mat-type floor pressure sensor," *Advanced Science Letters*, vol. 9, no. 1, pp. 591–596, 2012.

[25] R. Vera-Rodríguez, N. W. Evans, R. P. Lewis, B. Fauve, and J. S. Mason, "An experimental study on the feasibility of footsteps as a biometric," in *European Signal Process Conference-Eusipco*, 2007.

[26] R. Vera-Rodríguez, R. P. Lewis, J. S. Mason, and N. W. Evans, "Footstep recognition for a smart home environment," *International Journal of Smart Home*, vol. 2, no. 2, pp. 95–110, 2008.

[27] G. R. Doddington, M. A. Przybocki, A. F. Martin, and D. A. Reynolds, "The NIST speaker recognition evaluation–overview, methodology, systems, results, perspective," *Speech Communication*, vol. 31, no. 2, pp. 225–254, 2000.

[28] R. Subban and D. P. Mankame, "A study of biometric approach using fingerprint recognition," *Lecture Notes on Software Engineering*, vol. 1, no. 2, 2013.

[29] S. Sheela and P. Vijaya, "Iris recognition methods-survey," *International Journal of Computer Applications*, vol. 3, no. 5, pp. 19–25, 2010.

[30] S. Al-Obaidi, J. C. Wall, A. Al-Yaqoub, and M. Al-Ghanim, "Basic gait parameters: A comparison of reference data for normal subjects 20 to 29 years of age from kuwait and scandinavia," *Journal of rehabilitation research and development*, vol. 40, no. 4, pp. 361–366, 2003.

[31] D. Zhang, Y. Wang, and Z. Zhang, "Ethnicity classification based on a hierarchical fusion," in *Biometric Recognition*. Springer, 2012, pp. 300–307.

[32] D. S. Matovski, M. S. Nixon, S. Mahmoodi, and J. N. Carter, "The effect of time on gait recognition performance," *Information Forensics and Security, IEEE Transactions on*, vol. 7, no. 2, pp. 543–552, 2012.

[33] D. Gafurov, E. Snekkenes, and P. Bours, "Spoof attacks on gait authentication system," *Information Forensics and Security, IEEE Transactions on*, vol. 2, no. 3, pp. 491–502, 2007.

[34] B. B. Mjaaland, P. Bours, and D. Gligoroski, "Walk the walk: attacking gait biometrics by imitation," in *Information Security*. Springer, 2011, pp. 361–380.

978-1-4799-1737-2/15/$31.00 ©2015 IEEE